A model of the interface charge and chemical noise due to surface reactions in Ion Sensitive FETs

Leandro Julian Mele*‡, Pierpaolo Palestri* and Luca Selmi†
*DPIA, University of Udine, 33100, Udine, Italy.
†DIEF, University of Modena and Reggio Emilia, 44100, Modena, Italy.
‡Corresponding author. Email: mele.leandrojulian@spes.uniud.it

***Abstract*—We present a model of arbitrary chemical reactions at the interface between a solid and an electrolyte, aimed at computing the interface charge build-up and surface potential shift of ion-sensitive FETs in the presence of interfering ions. An expression for the rms value of the surface charge fluctuation and the resulting uncertainty in the ion concentration is derived as well. Application to nanoelectronic ISFET-based sensors for ions and proteins is demonstrated.**

***Index Terms*—ISFET, surface binding reactions, cross-sensitivity, charge fluctuations, chemical noise.**

I. Introduction

The sensing of ions and biomolecules using CMOS technology opens numberless possibilities of low-cost portable sensors for chemical screening [1], epigenetics [2] and has drastically cut the costs of DNA sequencing [3]. Physics-based modelling of the transduction mechanism provides useful insights for the optimization of the sensor sensitivity and signal-to-noise ratio. In DC potentiometric sensors, transduction takes place at the interface between a solid material and an electrolyte and the essential physics of such interface and its first order site-binding chemical reactions can be approximately described with commercial TCAD [4]. However, sensitivity to a given ion is affected by the presence of interfering ions; since TCAD uses electrons and holes to mimic ions, it cannot describe complex electrolytes and surface reactions that involve multiple ions in a set of coupled equations [5].

In this paper, we derive expressions to account for complex interface reactions between ions and binding sites. The expression of the surface charge is coupled to the equilibrium Poisson-Boltzmann (PB) equation to obtain the corresponding potential variation. In addition, we derive a useful expression of the noise induced by chemical fluctuations (hereinafter simply chemical noise) due to the stochasticity of binding/unbinding events.

II. Model description

Consider the surface sites at the solid/liquid interface of an electrochemical Field Effect Transistor (FET) and assume they can interact with different ionic species dissolved in the electrolyte. The binding/unbinding with one charged species entails a change of the site's state and of its net charge. Each state, i, is thus characterized by a probability f_i (i.e. how many sites over the total are in such state) and a net signed number of elementary charges z_i which may be non-integer. The simplest binding reaction is the first-order Langmuir adsorption [6] shown in Fig. 1 which can be seen as the elementary constituent of a generic set of chemical reactions.

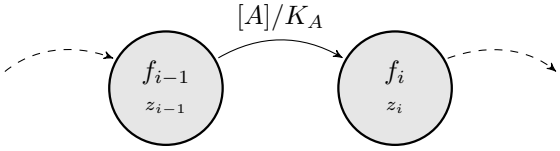

Fig. 1. Single arrow graph representing the steady state relationship between the $i-th$ state and the previous one, two arbitrary states of a site.

Here the site, from a complexed state $i-1$, binds the analyte A (whose volume concentration and dissociation constant of the reaction are $[A]$ and K_A respectively) leading to the complexed state i. In Fig. 1, nodes represent the states and the branches carry the coefficient that transforms one state probability with the previous when equilibrium is assumed. Reaction constants and ionic concentrations at the interface control the probability of the site to be in a given state and so the net surface charge expected at equilibrium.

A site with N configurations has $N-1$ reactions transforming one state into another. An extra equation is then given by the normalization of the f functions. This leads to a linear system with N equations and N unknowns:

$$\begin{cases} \vdots \\ f_i = \frac{[A]}{K_A} f_{i-1} \\ \vdots \\ \sum_{i=1}^{N} f_i = 1. \end{cases} \tag{1}$$

The surface charge density Q_S due to N_S identical sites per unit area interacting with the species, is

$$Q_S = qN_S \sum_{i=1}^{N} z_i f_i. \tag{2}$$

If different sites coexist, (1) and (2) should be solved for each site with the corresponding set of reactions, i.e. we have a matrix equation for each type of site. This general case is discussed in [7]. As for the electrostatics, if we assume equilibrium (i.e. the presence of at most one faradaic contact to the electrolyte [8]) and neglect steric effects, then the surface charge obviously influences the potential and the ionic distribution in the electrolyte according to the PB equations:

This work was supported by Italian MIUR and Flag-ERA through the project CONVERGENCE via the IUNET Consortium.

978-1-7281-0940-4/19/$31.00 ©2019 IEEE

$$\frac{d}{dx}\left[\varepsilon(x)\frac{d\psi(x)}{dx}\right] = -\left[\rho_m(x) + Q_{S,tot}\delta(x - x_S)\right] \quad (3)$$

$$\rho_m(x) = \sum_{l=1}^{N_{sp}} z_l q \left[\left[A_B^l\right] \exp\left(-\frac{z_l q}{k_b T}\psi(x)\right)\right] \quad (4)$$

where ε is the dielectric permittivity, ψ the electrostatic potential, $Q_{S,tot}$ is the sum of the surface charge densities of all different types of sites, z_l the $l-th$ ion/analyte net number of elementary charges, N_{sp} is the number of mobile species, $\left[A_B^l\right]$ the ion/analyte concentration in the bulk of the electrolyte. The interface ion concentrations depend on the voltage drop between the bulk of the electrolyte and the surface: a self-consistent solution of the coupled PB and the surface reaction equations is then necessary and has been implemented in this work.

III. Validation of the Model

Our general modelling approach reproduces special cases proposed in the literature, including the site-binding model (SB) [9] at the basis of pH sensing or the surface complexation of chloride ions described by the modified SB (mSB) model [10]. In our model, this modification yields an additional state, linked by a chemical reaction concerning a deprotonation plus the chloride binding. Figure 2 illustrates the good agreement between our implementation and the experiments in [10].

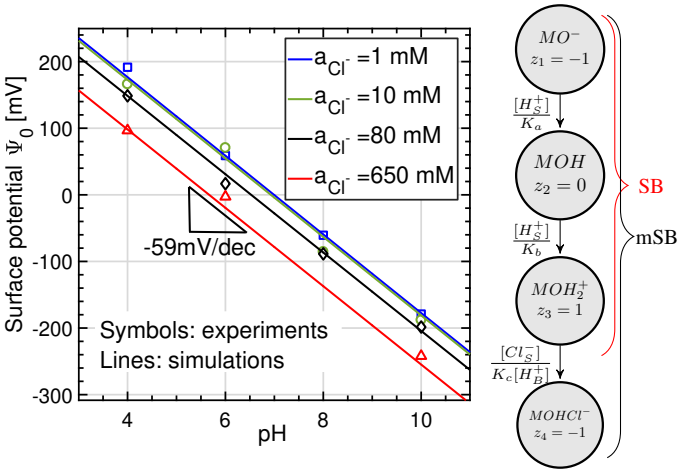

Fig. 2. Left: Comparison between our model and experiments from [10]. The parameters $K_a = 10^{-7}$ M, $K_b = 10^{-7}$ M $K_c = 3.3 \cdot 10^{-6}$ of the three chemical reactions and the number of sites $N_S = 10^{19}$ m^{-2} are taken from [10]. Right: SB and mSB reactions.

To prove that our approach can describe competing reactions, we compared our simulations with models found in the literature. The first one [11] was developed to estimate the surface charge generated at the gold/electrolyte interface of a sensor for the FimH protein. Here, the small oxidation of the gold surface leads to a pH response (SB) that electrostatically interferes with the attached mannoside ligands (Langmuir-like reactions), designed to capture FimH proteins.

Figure 3.a compares our simulations with the results obtained in [11] when using a constant double layer capacitance C_{DL} or the full PB model. We employ the same reaction parameters, number of hydroxyl groups per unit area and ionic

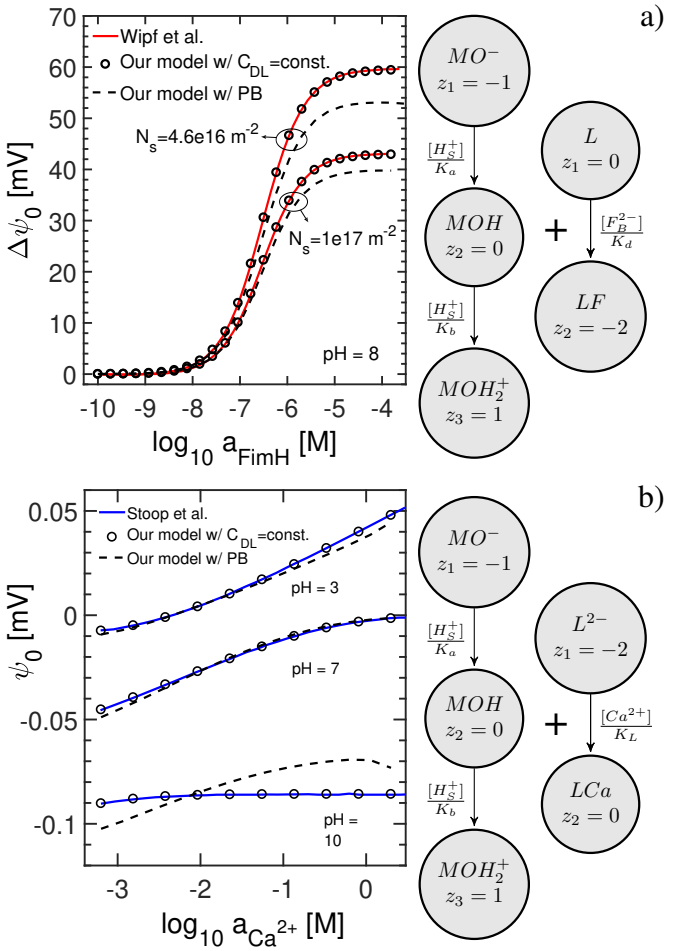

Fig. 3. Our model is applied to two cases of competing reactions using either the constant capacitance model and the full PB, and compared with results from the literature. In both cases the competing sites are SB and Langmuir-like reactions. a) Surface potential shift simulations for $C_{DL} = 0.1$ F/m^2 (symbols) and with the full PB equations (dashed lines) compared with the model in [11] (solid lines) for two densities of hydroxyl sites (SB). b) The surface potential is plotted versus $CaCl_2$ molar concentration for three different bulk pH values. Our model is compared with [12], using $C_{DL} = 0.16$ F/m^2.

strength as in the original work [11]. We find excellent agreement when embracing the same simplification as in [11] while the full PB solution predicts a lower plateau at high protein concentrations, likely because the ionic strength (especially at low concentrations such as in [11]) plays an important role in the C_{DL} which cannot be considered constant.

A second comparison is with the model in [12] for calcium Ca^{2+} sensing devices. Here the competing reactions are given by the SB model for the pH response and a Langmuir adsorption for the calcium sensing. To be consistent with the assumptions in [12], we consider the simple SB model instead of its modified version. The simulations have been performed both assuming a constant double layer capacitance, as in [12], and with the full PB system. Results are reported in Fig. 3.b. The comparison between the simplified (constant C_{DL}) and the more precise model shows that, once again, the assumption of constant double layer capacitance does not always hold true, as is here the case at high pH levels. The reason is that for large surface potentials the screening becomes more relevant and plays an important role while at low pH values the

two competing reactions counterbalance their charge resulting in small surface potential and thus smaller variations in the diffusive capacitance.

IV. Impact of Chemical Noise on pH Sensing

The discrete nature of binding/unbinding events due to surface reactions produces noise on the sensor response. Here we use our general approach to estimate the fluctuation coming from the stochastic nature of the binding interface, which results in an additional random telegraph noise superimposed to the 1/f noise from the oxide/silicon interface [13]. If we assume that the read-out circuit has a bandwidth larger than the reaction rates, the integrated noise is given by the RMS deviation of the surface charge Q_S from its average value. Using f_i from (1), this is

$$\sigma_{Q_S} = q\sqrt{\frac{N_S}{WL}\left[\sum_{i=1}^{N} z_i^2 f_i - \left(\sum_{i=1}^{N} z_i f_i\right)^2\right]}, \qquad (5)$$

where W and L are the dimensions of the sensing area.

Taking for instance an ion-sensitive-FET (ISFET) as sketched in Fig. 5.d, we convert the RMS value σ_{Q_S} in a voltage fluctuation and then in an error on the pH reading as illustrated in the block diagram of Fig. 4. Firstly, we consider the surface potential variation due to a small surface charge perturbation q_p added at the electrolyte/oxide interface and compute the function G that converts charge fluctuations into surface potential fluctuations. Then, we compute the ISFET sensitivity to the measured bulk pH, H and eventually estimate the RMS value of the pH fluctuation. Figure 5 plots H, G and σ_{Q_S} as a function of the pH computed solving the self-consistent PB equation in a 1D electrolyte/oxide structure (shown at the right). We see that H is larger for HfO_2 than for SiO_2 and almost perfectly Nernstian, ($H \approx 60mV/pH$) due to the larger number of sites ($10^{19}\mathrm{m}^{-2}$ [10] vs, $5 \cdot 10^{18}\mathrm{m}^{-2}$ [14]). At the same time, G is smaller for HfO_2. Therefore with HfO_2 the transfer function $|G/H|$ decreases but σ_{Q_S} increases. The net effect is that σ_{pH} is larger for SiO_2 than for HfO_2 (see, e.g., Fig. 6). The use of the mSB model for HfO_2 [10] (parameters for SiO_2 are not available to the best of our knowledge) results in changes of H and G and in an increase of σ_{Q_S} and σ_{pH}.

The estimation of the chemical noise can be relevant for instance for large arrays of pH sensors such as in the Ion Torrent platform for DNA sequencing [15]; in particular, the use of smaller and smaller μwells renders the binding more stochastic. Figure 6 shows the RMS value on the pH for different footprint areas (assuming sensing area = μwell area) and compares it to the signal the sensor should detect: dashed lines show the pH variation caused by a single proton inside the well, with the assumption that it diffuses towards the sensor surface. We see that σ_{pH_B} is negligibly small compared to single protonation events if the chamber is thin ($h = 1\ \mu\mathrm{m}$) but becomes comparable or larger for wells with larger footprint area devices while large areas require small well volume (thin well). The use of SiO_2 increases the chemical noise, and so does the account of the Cl^- ions (compare the SB and mSB models). Note that Figure 6 includes only the surface chemistry as noise source.

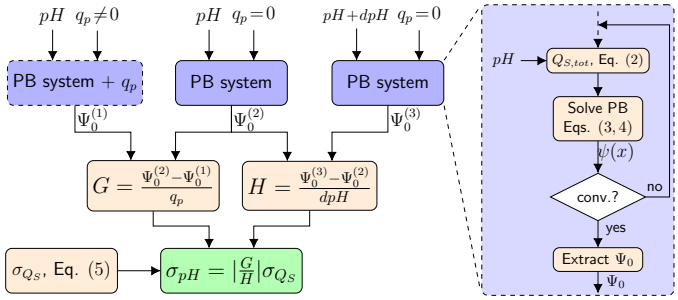

Fig. 4. Block diagram for the estimation of the chemical noise in an ISFET for pH sensing.

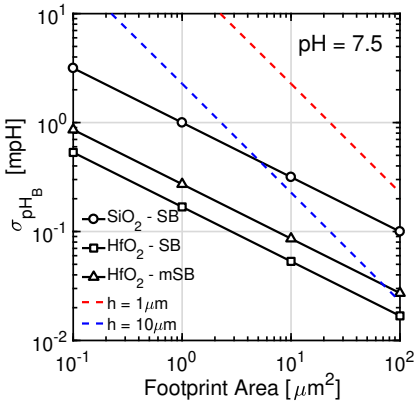

Fig. 6. RMS error of the pH for different sensing areas (symbols) for the three cases in Fig. 5. Dashed lines: variations induced by the addition of one proton, assuming heights of the μwell of 1 and 10 μm. pH and Cl concentration are from [16].

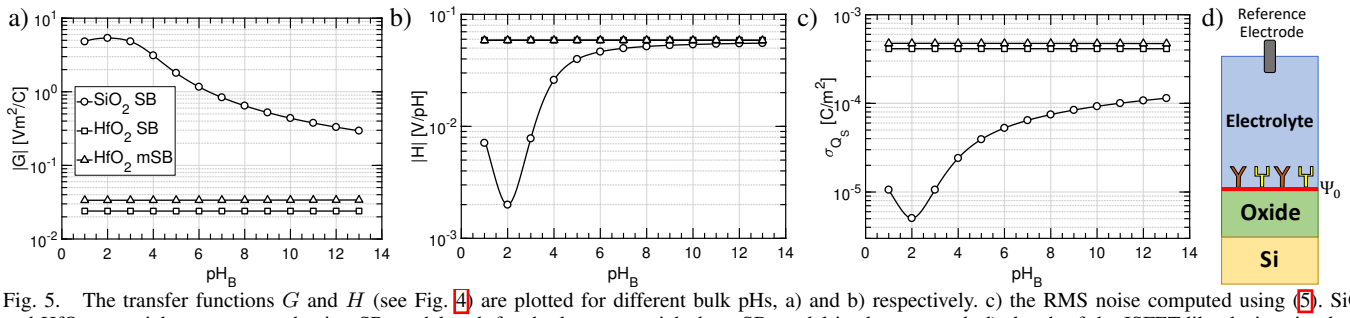

Fig. 5. The transfer functions G and H (see Fig. 4) are plotted for different bulk pHs, a) and b) respectively. c) the RMS noise computed using (5). SiO_2 and HfO_2 materials are compared using SB model and, for the latter material, the mSB model is also reported. d) sketch of the ISFET-like device simulated.

V. Charge fluctuation in competing reactions

We apply our model to competing reactions as in [17], where the same algorithm as in Fig. 4 holds with the analyte concentration in place of the pH. Here, the bovine serum albumin (BSA) is used as functionalization to sense its antibody (aBSA) at the nano-molar range of concentrations. These specific sites coexist with those typical of mSB. For simplicity, we consider all the binding reactions to take place at the same surface, thus neglecting the size of the proteins and the formation of a Donnan potential [18]. The computation of the net charge carried by BSA and aBSA is based on the pH and buffer ionic strength of the solution, as in [17]. Uniform spatial distribution of the charge inside the protein is assumed, and only the fraction within a Debye length is considered in our model. No Boltzmann distribution is used for aBSA protein since its dimensions are much larger than the Debye length [11]. We first fit the voltage shift experiments in [17] (Fig. 7); then, we evaluate the noise (Fig. 8). We see that chemical noise sets both a lower and an upper limit to the sensitivity when saturation is reached. Furthermore, smaller areas show progressively smaller range of usability.

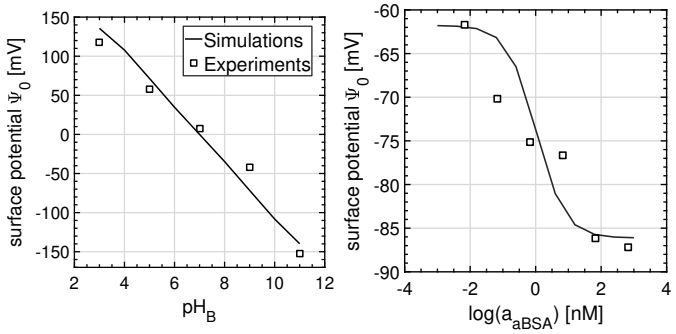

Fig. 7. Left: simulation of bare gold electrodes and data in [17] using K_a, K_b from [12] and K_c from [19]. Right: fit of the data with the addition of BSA/anti-BSA using $K_d = 1.2$ nM and $N_L = 1.7 \cdot 10^{16}$ m^{-2}.

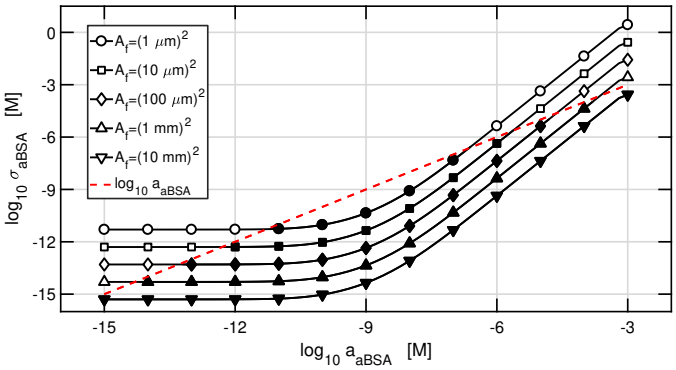

Fig. 8. Estimated RMS noise on the aBSA concentration for different sensing areas A_f. The red dashed line shows the relation $\sigma_{a_{aBSA}} = a_{aBSA}$. The filled symbols identify the useful operation range of the sensor.

VI. Conclusions

Our general model to compute the surface charge and chemical noise for arbitrary reactions at the biochemical sensor interface has been applied to ions and protein sensing. We found good agreement with existing ad-hoc models and went further analysing the chemical noise. Results suggest that the latter may play an important role in determining the useful range of potentiometric sensors.

References

[1] N. Moser, T. S. Lande, C. Toumazou, and P. Georgiou, "ISFETs in CMOS and emergent trends in instrumentation: A review," *IEEE Sensors J.*, vol. 16, no. 17, pp. 6496–6514, 2016. doi: 10.1109/JSEN.2016.2585920

[2] D. Ma *et al.*, "Adapting ISFETs for Epigenetics: An Overview," *IEEE Trans. Biomed. Circuits Syst.*, vol. 12, no. 5, pp. 1186–1201, Oct 2018. doi: 10.1109/TBCAS.2018.2838153

[3] M. Margulies *et al.*, "Genome sequencing in microfabricated high-density picolitre reactors," *Nature*, vol. 437, no. 7057, p. 376, 2005. doi: 10.1038/nature03959

[4] A. Bandiziol, P. Palestri, F. Pittino, D. Esseni, and L. Selmi, "A TCAD-Based Methodology to Model the Site-Binding Charge at ISFET/Electrolyte Interfaces," *IEEE Trans. Electron Devices*, vol. 62, no. 10, pp. 3379–3386, Oct 2015. doi: 10.1109/TED.2015.2464251

[5] F. Pittino, P. Palestri, P. Scarbolo, D. Esseni, and L. Selmi, "Models for the use of commercial TCAD in the analysis of silicon-based integrated biosensors," *Solid-State Electron.*, vol. 98, pp. 63–69, 2014. doi: 10.1016/j.sse.2014.04.011

[6] I. Langmuir, "The adsorption of gases on plane surfaces of glass, mica and platinum," *J. Am. Chem. Soc.*, vol. 40, no. 9, pp. 1361–1403, 1918. doi: 10.1021/ja02242a004

[7] L. J. Mele, P. Palestri, and L. Selmi, "General approach to model the surface charge and chemical noise induced by multiple surface reactions in potentiometric FET sensors," unpublished.

[8] A. J. Bard, L. R. Faulkner, J. Leddy, and C. G. Zoski, *Electrochemical methods: fundamentals and applications*. Wiley New York, 1980, vol. 2.

[9] D. E. Yates, S. Levine, and T. W. Healy, "Site-binding model of the electrical double layer at the oxide/water interface," *J. Chem. Soc. Farad. T. 1: Physical Chemistry in Condensed Phases*, vol. 70, pp. 1807–1818, 1974. doi: 10.1039/F19747001807

[10] A. Tarasov *et al.*, "Understanding the electrolyte background for biochemical sensing with ion-sensitive field-effect transistors," *ACS nano*, vol. 6, no. 10, pp. 9291–9298, 2012. doi: 10.1021/nn303795r

[11] M. Wipf *et al.*, "Label-Free FimH Protein Interaction Analysis Using Silicon Nanoribbon BioFETs," *ACS Sensors*, vol. 1, no. 6, pp. 781–788, 2016. doi: 10.1021/acssensors.6b00089

[12] R. L. Stoop *et al.*, "Competing surface reactions limiting the performance of ion-sensitive field-effect transistors," *Sensor. Actuat. B-Chem.*, vol. 220, pp. 500–507, 2015. doi: 10.1016/j.snb.2015.05.096

[13] E. Accastelli *et al.*, "Multi-Wire Tri-Gate Silicon Nanowires Reaching Milli-pH Unit Resolution in One Micron Square Footprint," *Biosensors*, vol. 6, no. 1, 2016. doi: 10.3390/bios6010009

[14] R. Van Hal, J. C. Eijkel, and P. Bergveld, "A general model to describe the electrostatic potential at electrolyte oxide interfaces," *Adv. Colloid. Interfac.*, vol. 69, no. 1-3, pp. 31–62, 1996. doi: 10.1016/S0001-8686(96)00307-7

[15] B. Merriman, I. T. R&D Team, and J. M. Rothberg, "Progress in Ion Torrent semiconductor chip based sequencing," *Electrophoresis*, vol. 33, no. 23, pp. 3397–3417, 2012. doi: 10.1002/elps.201200424

[16] J. Go and M. A. Alam, "The future scalability of pH-based genome sequencers: A theoretical perspective," *J. Appl. Phys.*, vol. 114, no. 16, p. 164311, 2013. doi: 10.1063/1.4825119

[17] A. Tarasov *et al.*, "Gold-coated graphene field-effect transistors for quantitative analysis of protein–antibody interactions," *2D Materials*, vol. 2, no. 4, p. 044008, nov 2015. doi: 10.1088/2053-1583/2/4/044008

[18] P. Bergveld, "A critical evaluation of direct electrical protein detection methods," *Biosens. Bioelectron.*, vol. 6, no. 1, pp. 55–72, 1991. doi: 10.1016/0956-5663(91)85009-L

[19] M. Wipf *et al.*, "Selective Sodium Sensing with Gold-Coated Silicon Nanowire Field-Effect Transistors in a Differential Setup," *ACS Nano*, vol. 7, no. 7, pp. 5978–5983, 2013. doi: 10.1021/nn401678u PMID: 23768238.